Published in final edited form as:
Basic Res Cardiol. 2011 November ; 106(6): 1123–1134. doi:10.1007/s00395-011-0201-0.

Coronary Arterioles in Type 2 Diabetic (db/db) Mice Undergo a Distinct Pattern of Remodeling Associated with Decreased Vessel Stiffness

Paige S. Katz[1,2], **Aaron J. Trask**[2], **Flavia M. Souza-Smith**[1,3], **Kirk R. Hutchinson**[2,3], **Maarten L. Galantowicz**[2], **Kevin C. Lord**[4], **James A. Stewart Jr.**[2], **Mary J. Cismowski**[2], **Kurt J. Varner**[3], and **Pamela A. Lucchesi**[2]

[1]Department of Physiology, Louisiana State University Health Sciences Center, New Orleans, Louisiana

[2]Center for Cardiovascular and Pulmonary Research and The Heart Center, The Research Institute at Nationwide Children's Hospital and Department of Pediatrics, The Ohio State University College of Medicine, Columbus, Ohio

[3]Department of Pharmacology and Experimental Therapeutics, Louisiana State University Health Sciences Center, New Orleans, Louisiana

[4]Feik School of Pharmacy, University of the Incarnate Word, San Antonio, Texas

Abstract

Background—Little is known about the impact of type 2 diabetes mellitus (DM) on coronary arteriole remodeling. The aim of this study was to determine the mechanisms that underlie coronary arteriole structural remodeling in type 2 diabetic (db/db) mice.

Methods and Results—Passive structural properties of septal coronary arterioles isolated from 12- and 16-wk-old diabetic db/db and control mice were assessed by pressure myography. Coronary arterioles from 12-wk-old db/db mice were structurally similar to age-matched controls. By 16-wks of age, coronary wall thickness was increased in db/db arterioles ($p < 0.01$), while luminal diameter was reduced (Control: 118±5μm; db/db: 102±4μm, $p < 0.05$), augmenting the wall-to-lumen ratio by 58% (Control: 5.9±0.6; db/db: 9.5±0.4, $p < 0.001$). Inward hypertrophic remodeling was accompanied by a 56% decrease in elastic modulus ($p < 0.05$, indicating decreased vessel coronary wall stiffness) and a ~30% reduction in coronary flow reserve in diabetic mice. Interestingly, aortic pulse wave velocity and femoral artery incremental modulus were increased ($p < 0.05$) in db/db mice, indicating macrovascular stiffness. Molecular tissue analysis revealed increased elastin-to-collagen ratio in diabetic coronaries when compared to control and a decrease in the same ratio in the diabetic aortas.

Conclusions—These data show that coronary arterioles isolated from type 2 diabetic mice undergo inward hypertrophic remodeling associated with decreased stiffness and increased elastin-to-collagen ratio which results in a decreased coronary flow reserve. This study suggests that coronary microvessels undergo a different pattern of remodeling from macrovessels in type 2 DM.

Address for Correspondence: Pamela A. Lucchesi, PhD, Center for Cardiovascular and Pulmonary Research, The Research Institute at Nationwide Children's Hospital, 700 Children's Drive, W303, Columbus, OH 43205, Telephone: (614) 722-4969, Fax: (614) 722-4881, pamela.lucchesi@nationwidechildrens.org.

Disclosures: None.

Keywords

vascular complications; type 2 diabetes; coronary flow; remodeling; matrix

Introduction

Type 2 diabetes mellitus (DM) is associated with cardiovascular complications including stroke, coronary artery disease and end-organ damage [9, 58]. Studies in both human and experimental type 2 DM demonstrate changes in blood vessel structure and function that underlie retinopathy, nephropathy, coronary artery disease, myocardial infarction and stroke. Both micro- and macro-vasculopathies underlie these complications [9]. Although alterations in large vessel function have been relatively well studied, much less is known about the impact of type 2 DM on resistance arterioles, especially coronary microvessels. Most studies have been performed in the aorta, renal, and mesenteric resistance beds, which are likely to respond in a vascular bed-specific manner due to distinct patterns of receptor expression, redox-sensitive cascades, and mechanical properties [5, 21, 31, 50]. Studies focusing on coronary arterioles in type 2 DM or obesity have reported endothelial dysfunction, impaired vascular reactivity, and altered endothelial permeability resulting in defects in flow-induced dilation and increased myogenic tone [2, 3, 6, 7, 18, 30, 32, 39].

Increasing evidence indicates that in addition to impaired function, structural remodeling of the blood vessel is an important determinant of microvessel function [20, 33]. Within the myocardium, changes in coronary arteriole structure can lead to decreased cardiac perfusion, reduced coronary flow reserve (CFR) and exacerbation of myocardial ischemia and injury. Evidence from clinical and experimental studies shows that CFR in diabetic patients is reduced, which can lead to ischemic events when faced with increased myocardial demand during exercise or exertion [34, 36, 56]. It is well known that diabetics have twice the risk of heart disease related death due to complications such as myocardial infarction [9, 22]. Clinical analysis of post-mortem cardiac samples also demonstrated increased medial thickness of coronary arterioles in type 2 DM patients [45].

The overall pattern of vessel wall remodeling depends on cellular and molecular mechanisms dictating vascular wall composition and these processes have not been extensively studied in diabetic coronary arterioles. Vessel remodeling results from dynamic changes in structural and cellular components of the vessel wall and involves changes in vascular smooth muscle cell (VSMC) growth, extracellular matrix (ECM), and cell-ECM interactions. The impact of these processes on lumen diameter depends upon the type of remodeling. Eutrophic remodeling involves the reorganization of existing cells and tissue, resulting in either a reduced (inward) or increased (outward) lumen diameter, but no change in VSMC growth or vessel cross-sectional area (CSA) [33]. On the other hand, hypertrophic remodeling results from an increase in VSMC growth or vessel CSA and can either be inward or outward [20, 33]. The goal of the present study was to determine whether type 2 DM impacts coronary arteriole structural remodeling and coronary flow reserve.

Methods

Mouse model

Experiments were performed on 12- and 16-wk male homozygous diabetic (db/db, BKS.Cg-*m* +/+*Lepr*^{db}/J) and age-matched heterozygote non-diabetic (Control, BKS.Cg-*m* +/+*Lepr*^{db}/J) mice obtained from Harlan Laboratories (Indianapolis, IN). The db/db mouse develops overt obesity and type 2 DM by 6–8 weeks of age, and therefore is a suitable model for these studies [10, 26]. Heterozygous mice were used as controls, since our preliminary studies

indicated that coronary arterioles isolated from these mice were not morphologically or physiologically different from wild type mice, C57BLKS/J (data not shown). Mice were housed under a 12-hr light/dark cycle at 22°C and 60% humidity. They were allowed *ad libitum* access to water and standard laboratory mouse chow. This study was conducted in accordance with National Institutes of Health Guidelines and was approved by the Institutional Animal Care and Use Committees of Louisiana State University Health Sciences Center and The Research Institute at Nationwide Children's Hospital.

Glucose Measurements

Mice were fasted for 8-hrs during the light cycle and blood was drawn from the tail vein. Blood glucose was measured using the Accu-Chek Advantage meter (Roche, Indianapolis, IN).

Blood Pressure Measurements by Telemetry

Mice were anesthetized using 2% isoflurane, vaporized with 100% oxygen. The right common carotid artery was isolated and cannulated with a blood pressure catheter connected to a radio telemetry transmitter (Model #PA-C10, Data Sciences, St. Paul, MN). Data collection began following the return of normal diurnal blood pressure cycle (7–10 days post surgery). Arterial pressure was monitored in conscious, freely moving mice. Data were collected using Transoma Medical Dataquest acquisition software (Data Sciences, St. Paul, MN) and was recorded for 10 secs every 15 mins for a total of 4 wks at 250 Hz. Data were averaged over 24-hr periods.

Preparation of Coronary Arterioles

Mice were anesthetized using 2% isoflurane, vaporized with 100% oxygen. The heart was excised and dissected in 4°C physiologic salt solution (PSS) composed of the following (in mM): 130 NaCl, 4 KCl, 1.2 $MgSO_4$, 4 $NaHCO_3$, 10 HEPES, 1.2 KH_2PO_4, 5 glucose, and 2.5 $CaCl_2$ at pH 7.4. Septal coronary arterioles (<120 μm internal diameter) at the level of the superior papillary muscle were isolated, excised and mounted onto 2 glass microcannulas within a pressure myograph chamber (Living Systems, Burlington, VT). One vessel was isolated per animal. Prior to any measurements, vessels were equilibrated for 30 mins under constant intraluminal pressure (50 mmHg) at 37°C in PSS. Internal diameter and left and right wall thickness were continuously monitored by a video image analyzer and data were recorded using WinDaq Lite (Dataq Instruments, Akron, OH) acquisition software.

Measurements of Coronary Arteriole Structure and Passive Mechanical Properties

All experiments were performed in Ca^{2+}-free PSS in the presence of 2 mM EGTA and 100μM sodium nitroprusside. A passive pressure-diameter curve was generated by increasing intraluminal pressure from 10 mmHg - 125 mmHg, and left and right wall thickness (WT) and internal diameters (D_i) were recorded at each pressure. This range of pressure encompasses the physiological range in these animals *in vivo* (see Table 2). The following structural and mechanical parameters were calculated:

$$\textit{External diameter}\ (D_e) = D_i + (2 \times WT)$$

$$\textit{Wall/lumen ratio} = (WT/D_i) \times 100$$

$$\textit{Cross Sectional Area}\,(\mathrm{CSA}) = \pi\,(D_e^{\,2} - D_i^{\,2})/4$$

$$\textit{Remodeling index} = 100 \times ((D_i)_C - (D_i)_{remodel})/((D_i)_C - (D_i)_d),$$

where $(D_i)_C$ and $(D_i)_d$ are the lumen diameters of the control and diabetic vessels, respectively.

$(D_i)_{remodel}$ represents the remodeled lumen

$$(D_i)_{remodel} = ((D_e)_d^{\,2} - 4\mathrm{CSA}_c/\pi)^{1/2},$$

where $(D_e)_d$ is the external diameter of the diabetic vessels and the CSA_c is the CSA of the control vessels.

$$\textit{Growth index} = (\mathrm{CSA}_c - \mathrm{CSA}_d)/\mathrm{CSA}_c$$

$$\textit{Circumferential Stress}\,(\sigma) = (P \times D_i)/(2\mathrm{WT}),$$

where P is pressure in dynes per square centimeter, D_i is the internal diameter for a given intraluminal pressure and WT is the wall thickness for a given intraluminal pressure.

$$\textit{Circumferential Strain}\,(\varepsilon) = (D_i - D_0)/D_0,$$

where D_i is the internal diameter for a given intraluminal pressure and D_0 is the reference diameter measured at 10 mmHg of intraluminal pressure.

$$\textit{Young's elastic modulus}\,(\mathrm{E}) = \mathrm{stress}\,(\sigma)/\mathrm{strain}\,(\varepsilon)$$

was used to determine arterial stiffness. However, since the stress-strain relationship is non-linear we also obtained the tangential or incremental elastic modulus (E_{inc}), or simply the slope of the stress-strain relationship (i.e. $\Delta\sigma/\Delta\varepsilon$).

Coronary Blood Flow

Coronary blood flow (CBF) was measured noninvasively with a high-frequency, high-resolution ultrasound unit (Vevo2100, Visual Sonics, Toronto, Canada) equipped with a 30 MHz probe, at baseline and under conditions of maximum flow (hyperemia). Doppler measurement of the left anterior descending artery (LAD) diameter and flow were performed under a modified four chamber view. Mice were anesthetized with 2% isoflurane vaporized with 100% oxygen. Following induction, isoflurane was reduced to 1% to determine baseline coronary flow, and then increased to 3% to measure maximal coronary flow [23–25, 54]; alternatively we used adenosine infusion to elicit maximal hyperemic flow. Following baseline and 3% isoflurane-induced maximal CBF measurements, a 4 min

intravenous infusion of adenosine (0.14 mg/kg*min) in the tail vein was performed to compare the two methods using the same animal. Maximal CBF was measured during the third min of adenosine infusion [53]. Data were analyzed offline by one observer to eliminate inter-observer variability. CBF was calculated using the equation:

$$CBF\ (\mathrm{mL/\ min}) = ((\pi/4) \times D^2 \times \mathrm{VTI} \times \mathrm{HR})/1000$$

where D is the internal coronary diameter (in mm) measured in B-mode ultrasound images, VTI is the velocity-time-integral (in mm), or area under the curve of the Doppler blood flow velocity tracing, and HR is heart rate.

$$Coronary\ Flow\ Reserve\ (CFR) = \mathrm{CBF}_{\mathrm{hyperemia}}/\mathrm{CBF}_{\mathrm{baseline}}$$

where $\mathrm{CBF}_{\mathrm{hyperemia}}$ is the coronary flow measured during either 3% isoflurane administration or adenosine infusion.

Vascular Morphology and Vascular Wall Cell Counts

In a subset of animals (n=6 per group), hearts were perfusion fixed at a constant pressure (gravity-fed) with 60 mM KCl-buffered formalin. Paraffin-embedded hearts were sectioned (5–6 μm) for morphology (H&E staining) and VSMC nuclei were counted and averaged by two blinded individuals. For immunohistochemical detection of smooth muscle cells, anti-α-smooth muscle actin (1:500 dilution, Sigma) was used (4°C overnight). For secondary labeling goat anti-mouse Alexa-Fluor (1:1,000 dilution, Invitrogen, Carlsbad, CA) was used and sections were mounted and counter stained using Vectashield with DAPI (Vector Laboratories, Burlingame, CA).

RNA Isolation and quantitative PCR Analysis

In a separate group of mice, coronary arterioles were isolated from 15–20 control or db/db mice (16-wks of age), pooled and snap frozen in liquid nitrogen for a total n=5 per group. Due to extremely small tissue size and limited availability, pooling of the coronary arterioles was required to obtain sufficient amounts of RNA for only a few targets. Aortas were isolated from 6 control or 6 db/db mice (16-wks of age). Total RNA was prepared from coronary artery pools or from single aorta using the Qiagen Micro Array kit according to manufacturer's instructions (Qiagen, Germantown, MD). Briefly, tissue was thawed in Qiazol reagent, then disrupted at 4°C by repeated sonication. Aqueous phases were removed following chloroform addition and centrifugation, and RNA was isolated on mini spin columns. An on-column DNAse digestion was performed as per instructions. All samples were eluted with nuclease-free water and RNA quantitated using a nano-drop spectrophotometer (Thermo, Waltham, MA). One microgram total RNA for each sample was reverse transcribed using the Fermentas RevertAid kit and protocol. Equivalent control reactions lacking reverse transcriptase were also performed. Quantitative PCR reactions were performed in duplicate using primer/universal probe sets designed via the Roche Applied Science website (https://www.roche-applied-science.com/sis/rtpcr/upl/index; see Table 1). All PCR reactions (25 μl) were performed on an Eppendorf Mastercycler ep realplex in opaque 96-well plates (Abgene, Epsom, United Kingdom) using the equivalent of 50 ng starting RNA, 200 nM forward and reverse primer, 250 nM probe and 1x Maxima Probe/ROX qPCR master mix (Fermentas, Glen Burnie, MD). Amplification parameters were as follows: 95°C, 10 min (x1); 95°C, 15 sec, 60°C, 1 min (x40). Ct values were determined after normalizing thresholds and allowing for drift correction. Relative

expression was determined using the DDC(T) methodology [44] normalizing to 60S ribosomal protein L13a (RPL13a).

Aortic Pulse Wave Velocity

In another subset of mice (n=5 per group), mice were anesthetized with 2% isoflurane and two mikro-tip pressure catheters (1F, Millar Instruments, Huston, TX) were inserted into the carotid and femoral arteries and advanced into the thoracic and abdominal aorta, respectively. After a 30-min equilibration period, blood pressure from each catheter was simultaneously recorded using LabScribe 2 software (iWORX, Dover, NH) and the time delay between the thoracic and abdominal aorta pressure waveforms was measured at the start of systole in 4 consecutive cardiac cycles. The distance between the two mikro-tip catheter transducers was carefully measured after sacrifice using 4–0 silk. Pulse wave velocity (PWV) was calculated by dividing the distance between catheter transducer tips by the time delay between pulse waves (represented in cm/ms).

Statistics

All data are represented as mean ± SEM with a probability of $p<0.05$ used for significance. Coronary structural measurements and calculations were analyzed using two-way repeated measures ANOVA followed by a post-hoc Boneferroni test. All other measurements were analyzed using an unpaired student's t-test using Prism 5.0 (GraphPad, LaJolla, CA).

Results

Body Weight, Blood Glucose, Blood Pressure and Heart Rate Measurements

At both 12- and 16-wks of age, db/db mice had significantly higher body weight and fasting blood glucose compared to controls (Table 2). Diastolic and systolic blood pressures and heart rate were not significantly different between control and db/db mice at 16-wks of age (Table 2).

Septal Coronary Arteriole Structure

We first examined passive coronary arteriole structure in 12-wk db/db mice, a time point at which endothelial dysfunction has been reported [2, 18]. There were no significant differences in internal diameter, wall thickness, wall-to-lumen ratio, or medial CSA between control and diabetic mice at 12-wks (Table 3). However, arteriole remodeling was evident in 16-wk db/db mice compared to age matched controls. The structure of coronary arterioles at 16-wks is depicted by H&E staining (Fig. 1). Passive vascular structural properties and mechanics were studied by progressively increasing intraluminal pressure. Using this method, luminal diameter was significantly reduced in db/db mice (n=10) compared to controls (n=8) over a range of pressures (Fig. 2a) while wall thickness was significantly increased (Fig. 2b). The media-to-lumen ratio was greater in db/db mice (Fig. 2c) and there was a trend towards an increase in medial CSA that did not reach statistical significance (Fig. 2d, $p = 0.09$).

Remodeling Index, Growth Index, and Vascular Wall Cell Number

We determined the type of remodeling occurring in the diabetic coronary arterioles by two different indices, remodeling and growth, and by quantifying the number of VSMCs within the vascular wall. We observed both an increase in the remodeling index and the growth index, which are represented as % change compared to control mice (Fig. 3a). In addition, db/db mice had an increased number of VSMCs within the vascular wall, which was normalized to the medial CSA to account for the amount of material in the vessel wall (Fig. 3b).

Septal Coronary Arteriole Mechanics

We furthered assessed vascular wall mechanics by comparing the stress-strain curves for diabetic and control coronary arterioles. The stress-strain curve calculated from diabetic coronary arterioles was shifted to the right compared to control arterioles (Fig. 4a), indicating decreased arterial wall stiffness. Direct calculations of E_{inc} over a range of physiological pressures, a geometry-independent measurement, confirmed the reduction in arterial stiffness as indicated by the stress-strain curve in db/db coronary arterioles (Fig. 4b).

Coronary Blood Flow

CBF was recorded at baseline (1% isoflurane) and at hyperemia-induced maximal flow (using either 3% isoflurane or adenosine infusion, Fig. 5a). We observed significant decreases in both basal and maximal hyperemic CBF in diabetic mice (Fig. 5b). Accordingly, db/db CFR was significantly reduced with isoflurane or adensoine administration (Fig. 5c).

Macrovascular Stiffness Measurements

Aortic stiffness was measured in 16-wk db/db (n=5) and control (n=5) mice by measuring PWV using two pressure catheters placed in the thoracic aorta and the abdominal aorta. Compared to control, db/db aorta showed increased PWV confirming increased aortic macrovascular stiffness (Fig. 6a–b). In addition, using pressure myography, femoral stiffness was increased as indicated by E_{inc} over a range of physiological pressures from 75–125 mmHg (Fig. 6c).

mRNA Expression of Elastin and Collagen I in Coronary Arterioles and Aorta

qtPCR analysis was used to examine the expression profiles of elastin and Alpha-1 type1 collagen (col1a1). Elastin mRNA expression was significantly increased in septal coronary arterioles of 16-wk diabetic mice compared to age-matched controls (n=5 of 6–10 pooled coronary arterioles for each group). Conversely, col1a1 was unchanged in the coronary arterioles isolated from diabetic mice (Fig. 7a). Interestingly, we observed a decrease in elastin mRNA with no change in col1a1 in diabetic aorta (n=6 for each group) by mRNA analysis (Fig. 7b), indicating a decrease in the elastin-to-collagen type 1 ratio.

Discussion

This study is the first to report that diabetic coronary arterioles in db/db mice undergo inward hypertrophic remodeling at 16-wks of age that is associated with *reduced* coronary vessel wall stiffness and reduced maximal CBF *in vivo*. Conversely, aortic PWV in the same diabetic animals were accelerated and E_{inc} in femoral arteries was increased. Both of these indices indicate increased stiffness of large conduit arteries in db/db mice. Collectively, these results document a unique pattern of vessel remodeling in the diabetic coronary microvasculature that differs from macrovessels such as that of the aorta and femoral artery, shown in this and other studies [46, 48]. This distinct pattern of microvascular remodeling was accompanied by changes in the elastin-to-collagen ratio: an increase in elastin expression in coronary arterioles, decreased elastin expression in the aorta, and no changes in collagen type 1 in either vascular bed.

There have been virtually no studies of vessel structure in coronary arterioles in type 2 DM. Traditionally, studies in this vascular bed focus on altered vasoreactivity and function [3, 30]. Endothelial dysfunction is an early indicator of vascular complications associated with type 2 DM [13, 14] and results, in part, from decreased nitric oxide bioavailability [38, 40]. Endothelial dysfunction in coronary arterioles from db/db mice occurs as early as 12-wks [2, 7, 18, 39]. Bagi et al. demonstrated endothelial dysfunction and impaired endothelium

dependent vasodilation in db/db mice at 12-wks [2], while Zhang's group documented a role for TNF-α, protease-activated receptor-2 (PAR-2) and the NAD(P)H oxidases in diabetic coronary arteriole dysfunction [18, 39].

Clinical and experimental studies examining type 2 DM-induced vascular remodeling are limited to non-coronary vascular beds, such as conduit arteries or small peripheral arteries. Rizzoni et al. [42] demonstrated hypertrophic remodeling (increased wall thickness and wall-to-lumen ratio) of small arteries isolated from gluteal biopsies of diabetic patients. Conversely, Crijins et al. [12], reported outward remodeling (increased lumen diameter without a change in medial-cross sectional area) in rat mesenteric resistance arteries of STZ-treated rats. Other studies of small arteries from type 2 DM animals revealed disparate results, including hypertrophic remodeling, decreased lumen diameter, or increased distensibility with no net growth [1, 42, 45]. We observed eutrophic outward remodeling in db/db mesenteric resistance arterioles (Souza-Smith et al., manuscript submitted). Thus it is likely that the type of vessel remodeling in response to type 2 DM is unique to each vascular bed, and may be ultimately dependent upon the local hemodynamic, neurohormonal, and inflammatory environment.

Our studies show that diabetic coronary arterioles display a distinct pattern of inward hypertrophic remodeling at 16-wks defined by a decrease in lumen diameter and increases in wall thickness and the wall-to-lumen ratio. Although the increase in medial CSA did not reach statistical significance, the 28% increase in growth index and the 62% increase in remodeling index are consistent with inward hypertrophic remodeling. The increase in wall thickness may be partially explained by an increased number of medial VSMCs. This overall pattern of inward hypertrophic remodeling is reminiscent of that observed in hypertensive small resistance arteries [27]. However, since there was no change in arterial blood pressure between db/db and control mice at 16-wks, the observed coronary artery remodeling is blood pressure independent. This finding is in agreement with a recent study be Schofield et al. [45] demonstrating that small arteries obtained from type 2 DM patients exhibited both an increased wall thickness and wall-to-lumen ratio that were not further increased in a subset of diabetic patients with hypertension.

We next determined whether the structural remodeling of the diabetic coronary arterioles was associated with changes in the passive mechanical properties of the vessel wall. Circumferential wall stress was decreased in db/db coronary arterioles, which resulted from increased wall thickness. Surprisingly, the diabetic coronary arterioles were less stiff, as measured by E_{inc} and the stress-strain relationship. These findings are contradictory to that observed in diabetic macrovessels such as the aorta and carotid arteries where diabetes-induced collagen modifications lead to increased vascular wall stiffness [41]. Our findings are in agreement with those reported in small arteries (from subcutaneous gluteal biopsies) from hypertensive patients in which decreased stiffness was demonstrated by a decreased elastic modulus [27]. A similar pattern of stiffness was also reported in cerebral arterioles from hypertensive rats [4].

Type 2 DM in the db/db model is due to leptin receptor (lepR) deficiency. Leptin signaling promotes VSMC growth *in vitro* [47] and deficiencies in either leptin or its receptor limit neointimal growth following arterial injury [8]. However, we observed both increased medial thickness (Fig. 2b) and VSMC number (Fig. 3b) in db/db coronary arterioles, suggesting that VSMC growth occurred despite leptin receptor deficiency. We cannot rule out the possibility that the decreased mechanical stiffness was secondary to leptin receptor defects. To address this concern, we used *in vivo* aortic PWV as a clinically relevant index of aortic stiffness. Aortic PWV was increased in db/db aorta, indicating increased wall stiffness (Fig. 6a–b). In addition, using pressure myography, E_{inc} was increased in diabetic

femoral arteries (Fig. 6c). Since conduit artery stiffness has been routinely reported in both animal models of diabetes and human diabetic patients, these results indicate that type 2 DM rather than LepR deficiency is responsible for the distinct changes in mechanical properties between macrovessels vs. microvessels in db/db mice. This conclusion is further supported by preliminary studies in the leptin-LepR-independent Ossabaw pig type 2 DM model, in which we also observed inward hypertrophic coronary arteriole remodeling and reduced mechanical stiffness (Trask et al., unpublished observations).

The exact molecular mechanisms that regulate these distinct differences in remodeling and mechanical properties are unknown. In general, changes in passive biomechanical properties of the vessel wall and vessel stiffness are determined by the content and composition of the ECM (collagen, elastin) and in VSMC function (see Stehouwer and Ferriera [49] for a comprehensive review). Alterations in fibronectin, elastin, and profibrotic regulatory molecules and matrix regulating enzymes influence overall vessel stiffness. ECM remodeling is influenced by both hemodynamic forces as well as extrinsic factors, such as hyperglycemia, renin-angiotensin system (RAS), cytokines and growth factors [57]. Both processes are dictated by a complex interplay between growth factors, vasoactive agents, increased reactive oxygen species (ROS) production, and advanced glycation end-products (AGEs) [20]. It is likely that the net impact of these processes may differ in coronary versus non-coronary arterioles. For example, coronary VSMC have much higher proliferative and migratory properties compared to femoral artery VSMC [28, 35].

In the present study, we were able to reliably measure two mRNA targets (elastin and collagen) from pooled coronary arterioles despite very limited amounts of tissue. Accordingly, we found that decreased coronary arteriole stiffness was associated with an increase in the ratio of elastin-to-collagen mRNA expression, while increased aortic stiffness was associated with a decreased ratio of elastin-to-collagen mRNA expression. Since we observed no differences in collagen type 1 mRNA expression between db/db and control mice in either vascular bed, the changes in the ratio reflect reciprocal changes in elastin. Conversely, Garcia and Kassab reported concomitant increases in both elastin and collagen in stiffer right coronary conduit arteries in pigs subjected to right ventricular hypertrophy, although a disproportionate increase in collagen reduced the elastin-to-collagen ratio by about half [19]. The small amount of tissue obtained from coronary arterioles (<1μg per vessel) prevented us from performing a more comprehensive analysis of the ECM protein expression. However, it is generally accepted that there is a direct correlation between steady-state elastin mRNA levels and elastin protein synthesis and secretion [17, 29, 43, 51]. It is possible that elastin degradation [16] or post-transcriptional repression through microRNA [37] could lead to a discrepancy between mRNA and protein levels. It is also likely that AGE- dependent collagen cross-linking contributes to increased arterial stiffness in the aorta and femoral artery, as shown by Levy's group [55]. Although beyond the scope of the present manuscript, future proteomic studies will allow us to more fully identify the molecular mechanisms that underlie vessel-specific remodeling.

While this structural remodeling is blood pressure independent, it is possible that myocardial mechanics affect the passive structural and biomechanical properties of coronary arterioles. Unlike surface coronary arteries, septal arterioles are embedded in cardiac muscle and therefore undergo repeated mechanical compression with each beat of the heart. During diastole the myocardial effect on the coronary arteries is small. However, Westerhof et al. describes two mechanisms during systole to explain how the contracting myocardium affects the coronary microvasculature: 1) During systole the contracting myocardium increases ventricular pressure, which increases intramyocardial pressure, which compresses the vasculature; 2) During contraction, cardiac muscle fibers shorten and increase their width, which affects the vasculature by reducing vessel lumen diameter due to compression [52].

Due to this increased extravascular pressure and myocardial contraction during systole, blood flows through the coronary circulation primarily during diastole. Kassab et al. demonstrated that the local mechanical environment of the left ventricle (i.e. increased loading and increased intramyocardial pressure) resulted in differences in coronary vessel medial thickness [11]. Moreover, left ventricular diastolic stiffness is increased in db/db mice, largely due to increased AGE-dependent collagen cross-linking (Stewart et al., manuscript submitted). Since intravascular pressure (blood pressure) was not different between control and db/db mice, as measured by radio telemetry, and db/db coronary arterioles are exposed to higher extravascular forces from the stiffer myocardium, it is tempting to speculate that the inward hypertrophic remodeling and increase wall thickness occurs as an attempt to normalize transmural wall stress. In other words, the decreased stiffness may occur in order to buffer the effects of greater extravascular pressure in type 2 diabetic hearts, in order to limit medial wall stress. In this scenario, the increased VSMC number would not only decrease wall stress by increasing medial thickness but also by deceasing stiffness since VSMC are considered to be more distensible than collagen [27].

In order to determine the functional significance of coronary arteriole remodeling, we directly measured basal and maximal CBF by non-invasive transthoracic high-frequency pulse wave Doppler imaging. Although fluorescence microspheres are the gold standard for quantitatively measuring flow [53], more recently, noninvasive imaging by Doppler is used to measure both basal and maximal CBF over time in the same animal without the requirement of taking reference blood samples or insertion of catheters for microsphere delivery (see [23] for a recent review). Two different methods were used to achieve maximal hyperemia, adenosine infusion and a transient increase in isoflurane (1% to 3%); both methods yielded similar values in maximal CBF. Since both methods are independent of endothelial function, it is unlikely that changes in flow-mediated dilation account for the difference between groups. Moreover, our values obtained for CBF are in keeping with previous reports [24, 54]. We observed a significant reduction in basal CBF in diabetic mice, and there was a significant decrease in maximal CBF in db/db mice, suggesting vascular impairment at maximum dilation. Direct calculations of CFR using maximal hyperemic and basal CBF revealed a significant impairment in CFR in diabetic mice. While basal CBF is regulated by a variety of factors including metabolic, myogenic, and endothelial cell mediated mechanisms, maximal CBF is largely dependent on total coronary resistance which is the sum of both passive (structural) and active (smooth muscle tone) components [15]. We cannot rule out potential effects of cardiac contraction on microcirculatory resistance, although these effects have been reported to be minimal during diastole [52]. Since we did not simultaneously measure pressure and flow, we were unable to directly assess the contribution of pulse pressure to the changes in CFR. Taken together, our results suggest a good correlation between coronary arteriole structural remodeling and reduced CBF and CFR.

In summary, our data show inward hypertrophic remodeling of coronary arterioles isolated from 16-wk type 2 diabetic mice that is associated with a decrease in vascular wall stiffness and reduced CBF and CFR. Future studies are necessary to determine the molecular mechanisms that account for these changes in microvascular remodeling as well as the relative contribution of neurohormonal agents, inflammation, hyperglycemia and insulin resistance in coronary remodeling.

Acknowledgments

Funding

This research was supported by NIH COBRE P20RR18766 (LSUHSC), NIH 2R01HL056046 and 2R01HL63318 (PAL), T32HL098039 (AJT), and The Heart Center at Nationwide Children’s Hospital.

References

1. Bagi Z, Erdei N, Toth A, Li W, Hintze TH, Koller A, Kaley G. Type 2 diabetic mice have increased arteriolar tone and blood pressure: enhanced release of COX-2-derived constrictor prostaglandins. Arterioscler Thromb Vasc Biol. 2005; 25:1610–1616.10.1161/01.ATV.0000172688.26838.9f [PubMed: 15947245]
2. Bagi Z, Koller A, Kaley G. Superoxide-NO interaction decreases flow- and agonist-induced dilations of coronary arterioles in Type 2 diabetes mellitus. Am J Physiol Heart Circ Physiol. 2003; 285:H1404–1410.10.1152/ajpheart.00235.2003 [PubMed: 12805026]
3. Bassenge E, Heusch G. Endothelial and neuro-humoral control of coronary blood flow in health and disease. Rev Physiol Biochem Pharmacol. 1990; 116:77–165. [PubMed: 2293307]
4. Baumbach GL, Heistad DD. Remodeling of cerebral arterioles in chronic hypertension. Hypertension. 1989; 13:968–972. [PubMed: 2737731]
5. Beaucage P, Yamaguchi N, Lariviere R, Moreau P. Heterogeneity in the acute control of vascular protein synthesis in vivo. J Vasc Res. 2003; 40:123–131.10.1159/000070709.JVR2003040002123 [PubMed: 12808348]
6. Becker BF, Chappell D, Jacob M. Endothelial glycocalyx and coronary vascular permeability: the fringe benefit. Basic Res Cardiol. 2010; 105:687–701.10.1007/s00395-010-0118-z [PubMed: 20859744]
7. Belin de Chantemele EJ, Ali MI, Mintz J, Stepp DW. Obesity induced-insulin resistance causes endothelial dysfunction without reducing the vascular response to hindlimb ischemia. Basic Res Cardiol. 2009; 104:707–717.10.1007/s00395-009-0042-2 [PubMed: 19548058]
8. Bodary PF, Shen Y, Ohman M, Bahrou KL, Vargas FB, Cudney SS, Wickenheiser KJ, Myers MG Jr, Eitzman DT. Leptin regulates neointima formation after arterial injury through mechanisms independent of blood pressure and the leptin receptor/STAT3 signaling pathways involved in energy balance. Arterioscler Thromb Vasc Biol. 2007; 27:70–76.10.1161/01.ATV.0000252068.89775.ee [PubMed: 17095713]
9. Buse JB, Ginsberg HN, Bakris GL, Clark NG, Costa F, Eckel R, Fonseca V, Gerstein HC, Grundy S, Nesto RW, Pignone MP, Plutzky J, Porte D, Redberg R, Stitzel KF, Stone NJ. Primary prevention of cardiovascular diseases in people with diabetes mellitus: a scientific statement from the American Heart Association and the American Diabetes Association. Circulation. 2007; 115:114–126. CIRCULATIONAHA10.1161/CIRCULATIONAHA.106.179294. [PubMed: 17192512]
10. Chen H, Charlat O, Tartaglia LA, Woolf EA, Weng X, Ellis SJ, Lakey ND, Culpepper J, Moore KJ, Breitbart RE, Duyk GM, Tepper RI, Morgenstern JP. Evidence that the diabetes gene encodes the leptin receptor: identification of a mutation in the leptin receptor gene in db/db mice. Cell. 1996; 84:491–495.10.1016/S0092-8674(00)81294-5 [PubMed: 8608603]
11. Choy JS, Kassab GS. Wall thickness of coronary vessels varies transmurally in the LV but not the RV: implications for local stress distribution. Am J Physiol. 2009; 297:H750–758.10.1152/ajpheart.01136.2008
12. Crijns FR, Wolffenbuttel BH, De Mey JG, Struijker Boudier HA. Mechanical properties of mesenteric arteries in diabetic rats: consequences of outward remodeling. Am J Physiol. 1999; 276:H1672–1677. [PubMed: 10330253]
13. Dandona P, Aljada A, Chaudhuri A, Mohanty P. Endothelial dysfunction, inflammation and diabetes. Rev Endocr Metab Disord. 2004; 5:189–197. 0.1023/B:REMD.0000032407.88070.0a. [PubMed: 15211090]
14. Deedwania P, Srikanth S. Diabetes and vascular disease. Expert Rev Cardiovasc Ther. 2008; 6:127–138.10.1586/14779072.6.1.127 [PubMed: 18095912]
15. Duncker DJ, Bache RJ. Regulation of coronary blood flow during exercise. Phys Rev. 2008; 88:1009–1086.10.1152/physrev.00045.2006
16. Fonck E, Prod'hom G, Roy S, Augsburger L, Rufenacht DA, Stergiopulos N. Effect of elastin degradation on carotid wall mechanics as assessed by a constituent-based biomechanical model. Am J Physiol Heart Circ Physiol. 2007; 292:H2754–2763.10.1152/ajpheart.01108.2006 [PubMed: 17237244]

17. Franco C, Hou G, Ahmad PJ, Fu EY, Koh L, Vogel WF, Bendeck MP. Discoidin domain receptor 1 (ddr1) deletion decreases atherosclerosis by accelerating matrix accumulation and reducing inflammation in low-density lipoprotein receptor-deficient mice. Circ Res. 2008; 102:1202–1211.10.1161/CIRCRESAHA.107.170662 [PubMed: 18451340]
18. Gao X, Belmadani S, Picchi A, Xu X, Potter BJ, Tewari-Singh N, Capobianco S, Chilian WM, Zhang C. Tumor necrosis factor-alpha induces endothelial dysfunction in Lepr(db) mice. Circulation. 2007; 115:245–254.10.1161/CIRCULATIONAHA.106.650671 [PubMed: 17200442]
19. Garcia M, Kassab GS. Right coronary artery becomes stiffer with increase in elastin and collagen in right ventricular hypertrophy. J Appl Physiol. 2009; 106:1338–1346.10.1152/japplphysiol.90592.2008 [PubMed: 19179652]
20. Gibbons GH, Dzau VJ. The emerging concept of vascular remodeling. N Engl J Med. 1994; 330:1431–1438. [PubMed: 8159199]
21. Girardot D, Demeilliers B, deBlois D, Moreau P. ERK1/2-mediated vasoconstriction normalizes wall stress in small mesenteric arteries during NOS inhibition in vivo. J Cardiovasc Pharmacol. 2003; 42:339–347. [PubMed: 12960678]
22. Grundy SM, Benjamin IJ, Burke GL, Chait A, Eckel RH, Howard BV, Mitch W, Smith SC Jr, Sowers JR. Diabetes and cardiovascular disease: a statement for healthcare professionals from the American Heart Association. Circulation. 1999; 100:1134–1146.10.1161/01.CIR.100.10.1134 [PubMed: 10477542]
23. Hartley CJ, Reddy AK, Madala S, Entman ML, Michael LH, Taffet GE. Doppler Velocity Measurements from Large and Small Arteries of Mice. Am J Physiol Heart Circ Physiol. 2011 In Press. 10.1152/ajpheart.00320.2011
24. Hartley CJ, Reddy AK, Madala S, Michael LH, Entman ML, Taffet GE. Effects of isoflurane on coronary blood flow velocity in young, old and ApoE(-/-) mice measured by Doppler ultrasound. Ultrasound Med Biol. 2007; 33:512–521.10.1016/j.ultrasmedbio.2006.11.002 [PubMed: 17346873]
25. Hartley CJ, Reddy AK, Michael LH, Entman ML, Taffet GE. Coronary flow reserve as an index of cardiac function in mice with cardiovascular abnormalities. Conf Proc IEEE Eng Med Biol Soc. 2009; 1:1094–1097.10.1109/IEMBS.2009.5332488 [PubMed: 19963485]
26. Hummel KP, Dickie MM, Coleman DL. Diabetes, a new mutation in the mouse. Science. 1966; 153:1127–1128.10.1126/science.153.3740.1127 [PubMed: 5918576]
27. Intengan HD, Deng LY, Li JS, Schiffrin EL. Mechanics and composition of human subcutaneous resistance arteries in essential hypertension. Hypertension. 1999; 33:569–574.10.1161/01.HYP.33.1.569 [PubMed: 9931167]
28. Jin KL, Mao XO, Nagayama T, Goldsmith PC, Greenberg DA. Induction of vascular endothelial growth factor receptors and phosphatidylinositol 3′-kinase/Akt signaling by global cerebral ischemia in the rat. Neuroscience. 2000; 100:713–717.10.1016/S0306-4522(00)00331-6 [PubMed: 11036205]
29. Kuang PP, Zhang XH, Rich CB, Foster JA, Subramanian M, Goldstein RH. Activation of elastin transcription by transforming growth factor-beta in human lung fibroblasts. Am J Physiol Lung Cell Mol Physiol. 2007; 292:L944–952.10.1152/ajplung.00184.2006 [PubMed: 17209135]
30. Liu Y, Gutterman DD. Vascular control in humans: focus on the coronary microcirculation. Basic Res Cardiol. 2009; 104:211–227.10.1007/s00395-009-0775-y [PubMed: 19190954]
31. Martens FM, Demeilliers B, Girardot D, Daigle C, Dao HH, deBlois D, Moreau P. Vessel-specific stimulation of protein synthesis by nitric oxide synthase inhibition: role of extracellular signal-regulated kinases 1/2. Hypertension. 2002; 39:16–21.10.1161/hy0102.099025 [PubMed: 11799072]
32. Moien-Afshari F, Ghosh S, Khazaei M, Kieffer TJ, Brownsey RW, Laher I. Exercise restores endothelial function independently of weight loss or hyperglycaemic status in db/db mice. Diabetologia. 2008; 51:1327–1337.10.1007/s00125-008-0996-x [PubMed: 18437348]
33. Mulvany MJ, Baumbach GL, Aalkjaer C, Heagerty AM, Korsgaard N, Schiffrin EL, Heistad DD. Vascular remodeling. Hypertension. 1996; 28:505–506. [PubMed: 8794840]

34. Nahser PJ Jr, Brown RE, Oskarsson H, Winniford MD, Rossen JD. Maximal coronary flow reserve and metabolic coronary vasodilation in patients with diabetes mellitus. Circulation. 1995; 91:635–640.10.1161/01.CIR.91.3.635 [PubMed: 7828287]
35. Nishiguchi F, Fukui R, Hoshiga M, Negoro N, Ii M, Nakakohji T, Kohbayashi E, Ishihara T, Hanafusa T. Different migratory and proliferative properties of smooth muscle cells of coronary and femoral artery. Atherosclerosis. 2003; 171:39–47.10.1016/j.atherosclerosis.2003.08.007 [PubMed: 14642404]
36. Nitenberg A, Valensi P, Sachs R, Dali M, Aptecar E, Attali JR. Impairment of coronary vascular reserve and ACh-induced coronary vasodilation in diabetic patients with angiographically normal coronary arteries and normal left ventricular systolic function. Diabetes. 1993; 42:1017–1025.10.1016/j.coph.2006.01.001 [PubMed: 8513969]
37. Ott CE, Grunhagen J, Jager M, Horbelt D, Schwill S, Kallenbach K, Guo G, Manke T, Knaus P, Mundlos S, Robinson PN. MicroRNAs differentially expressed in postnatal aortic development downregulate elastin via 3′ UTR and coding-sequence binding sites. PLoS One. 2011; 6:e16250.10.1371/journal.pone.0016250 [PubMed: 21305018]
38. Pacher P, Szabo C. Role of peroxynitrite in the pathogenesis of cardiovascular complications of diabetes. Curr Opin Pharmacol. 2006; 6:136–141. [PubMed: 16483848]
39. Park Y, Yang J, Zhang H, Chen X, Zhang C. Effect of PAR2 in regulating TNF-alpha and NAD(P)H oxidase in coronary arterioles in type 2 diabetic mice. Basic Res Cardiol. 2011; 106:111–123.10.1007/s00395-010-0129-9 [PubMed: 20972877]
40. Pennathur S, Heinecke JW. Mechanisms for oxidative stress in diabetic cardiovascular disease. Antioxid Redox Signal. 2007; 9:955–969.10.108/ars.2007.1595 [PubMed: 17508917]
41. Reddy GK. AGE-related cross-linking of collagen is associated with aortic wall matrix stiffness in the pathogenesis of drug-induced diabetes in rats. Microvasc Res. 2004; 68:132–142.10.1016/j.mvr.2004.04.002 [PubMed: 15313123]
42. Rizzoni D, Porteri E, Guelfi D, Muiesan ML, Valentini U, Cimino A, Girelli A, Rodella L, Bianchi R, Sleiman I, Rosei EA. Structural alterations in subcutaneous small arteries of normotensive and hypertensive patients with non-insulin-dependent diabetes mellitus. Circulation. 2001; 103:1238–1244.10.1161/01.CIR.103.9.1238 [PubMed: 11238267]
43. Rosenbloom J. Elastin: relation of protein and gene structure to disease. Lab Invest. 1984; 51:605–623. [PubMed: 6150137]
44. Schmittgen TD, Livak KJ. Analyzing real-time PCR data by the comparative C(T) method. Nat Protoc. 2008; 3:1101–1108. [PubMed: 18546601]
45. Schofield I, Malik R, Izzard A, Austin C, Heagerty A. Vascular structural and functional changes in type 2 diabetes mellitus: evidence for the roles of abnormal myogenic responsiveness and dyslipidemia. Circulation. 2002; 106:3037–3043.10.1161/01.CIR.0000041432.80615.A5 [PubMed: 12473548]
46. Schram MT, Henry RM, van Dijk RA, Kostense PJ, Dekker JM, Nijpels G, Heine RJ, Bouter LM, Westerhof N, Stehouwer CD. Increased central artery stiffness in impaired glucose metabolism and type 2 diabetes: the Hoorn Study. Hypertension. 2004; 43:176–181.10.1161/01.HYP.000011829.46090.92 [PubMed: 14698999]
47. Shan J, Nguyen TB, Totary-Jain H, Dansky H, Marx SO, Marks AR. Leptin-enhanced neointimal hyperplasia is reduced by mTOR and PI3K inhibitors. Proc Natl Acad Sci U S A. 2008; 105:19006–19011.10.1073/pnas.0809743105 [PubMed: 19020099]
48. Sista AK, O'Connell MK, Hinohara T, Oommen SS, Fenster BE, Glassford AJ, Schwartz EA, Taylor CA, Reaven GM, Tsao PS. Increased aortic stiffness in the insulin-resistant Zucker fa/fa rat. Am J Physiol Heart Circ Physiol. 2005; 289:H845–851.10.1152/ajpheart.00134.2005 [PubMed: 15833807]
49. Stehouwer CD, Henry RM, Ferreira I. Arterial stiffness in diabetes and the metabolic syndrome: a pathway to cardiovascular disease. Diabetologia. 2008; 51:527–539.10.1007/s00125-007-0918-3 [PubMed: 18239908]
50. Urena J, Smani T, Lopez-Barneo J. Differential functional properties of Ca^{2+} stores in pulmonary arterial conduit and resistance myocytes. Cell Calcium. 2004; 36:525–534.10.1016/j.ceca.2004.05.005 [PubMed: 15488602]

51. Weissen-Plenz G, Eschert H, Volker W, Sindermann JR, Beissert S, Robenek H, Scheld HH, Breithardt G. Granulocyte macrophage colony-stimulating factor deficiency affects vascular elastin production and integrity of elastic lamellae. J Vasc Res. 2008; 45:103–110.10.1159/000109819 [PubMed: 17934321]
52. Westerhof N, Boer C, Lamberts RR, Sipkema P. Cross-talk between cardiac muscle and coronary vasculature. Phys Rev. 2006; 86:1263–1308.10.1152/physrev.00029.2005
53. Wikstrom J, Gronros J, Bergstrom G, Gan LM. Functional and morphologic imaging of coronary atherosclerosis in living mice using high-resolution color Doppler echocardiography and ultrasound biomicroscopy. J Am Coll Cardiol. 2005; 46:720–727.10.1016/j.jacc.2005.04.053 [PubMed: 16098442]
54. Wikstrom J, Gronros J, Gan LM. Adenosine induces dilation of epicardial coronary arteries in mice: relationship between coronary flow velocity reserve and coronary flow reserve in vivo using transthoracic echocardiography. Ultrasound Med Biol. 2008; 34:1053–1062.10.1016/j.ultrasmedbio.2007.12.004 [PubMed: 18313201]
55. Wolffenbuttel BH, Boulanger CM, Crijns FR, Huijberts MS, Poitevin P, Swennen GN, Vasan S, Egan JJ, Ulrich P, Cerami A, Levy BI. Breakers of advanced glycation end products restore large artery properties in experimental diabetes. Proc Natl Acad Sci USA. 1998; 95:4630–4634. [PubMed: 9539789]
56. Yokoyama I, Yonekura K, Ohtake T, Yang W, Shin WS, Yamada N, Ohtomo K, Nagai R. Coronary microangiopathy in type 2 diabetic patients: relation to glycemic control, sex, and microvascular angina rather than to coronary artery disease. J Nucl Med. 2000; 41:978–985. [PubMed: 10855621]
57. Zieman SJ, Melenovsky V, Kass DA. Mechanisms, pathophysiology, and therapy of arterial stiffness. Arterioscler Thromb Vasc Biol. 2005; 25:932–943.10.1161/01.ATV.0000160548.78317.29 [PubMed: 15731494]
58. Zimmet P, Alberti KG, Shaw J. Global and societal implications of the diabetes epidemic. Nature. 2001; 414:782–787.10.1038/414782a [PubMed: 11742409]

Clinical Perspective

Coronary artery disease is a common vascular complication of type 2 DM and a leading cause of morbidity and mortality. Although atherosclerosis and altered vasoreactivity are hallmarks of macrovascular and microvascular disease, respectively, little is known about the impact of structural remodeling on CBF and perfusion. Using leptin receptor deficient type 2 diabetic mice, we demonstrate that diabetic coronary arterioles undergo a unique pattern of structural remodeling that results in a decrease in luminal diameter and vessel stiffness that correlate with reduced CFR. These results raise the possibility that passive structural remodeling may contribute to the higher incidence of myocardial infarction and myocardial ischemia in type 2 diabetics [22]. We also document increased aortic flow velocities and increased femoral artery E_{inc}, confirming that increased stiffness of large conduit arteries typically found in diabetic patients. This may imply that current therapeutic strategies aimed at reduced arterial stiffness may not be optimal for treating the coronary microvasculature.

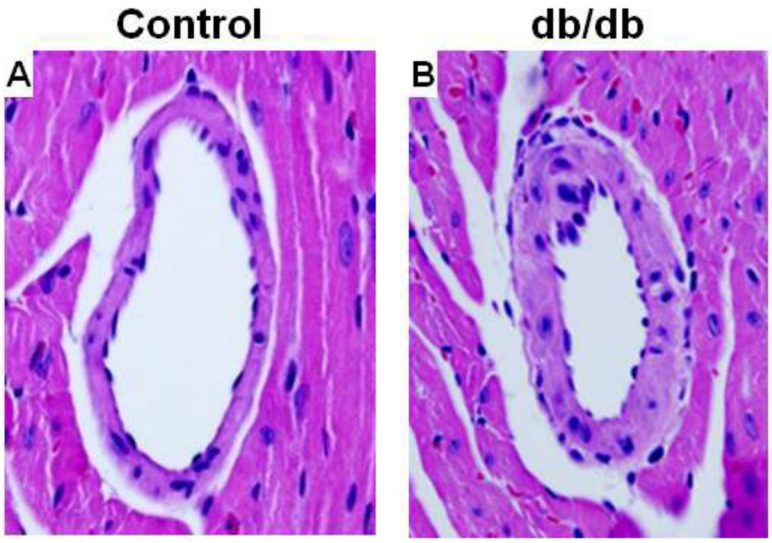

Fig. 1.

Hematoxylin and eosin-stained sections of septal coronary arterioles from 16-wk control **(a)** and db/db **(b)** mice at 60x magnification. Coronary artery structural remodeling was evident in 16-wk old db/db mice. Representative of n=4 mice per group.

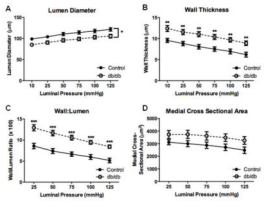

Fig. 2.

Passive structural measurements of isolated coronary arterioles from 16-wk diabetic and control mice. These measurements demonstrated decreased lumen diameter **(a)**, increased wall thickness **(b)**, increased wall-to-lumen ratio **(c)** and no change in medial CSA **(d)**. Values are mean SEM, * $p < 0.05$, ** $p < 0.01$, and *** $p < 0.001$vs. control.

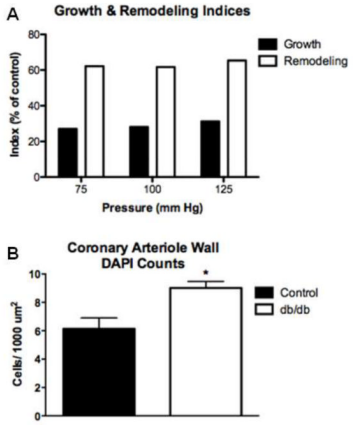

Fig. 3.

Increased remodeling index and decreased growth index of isolated coronary arterioles under physiological pressures of 75, 100 and 125 mmHg **(a)**. Note that these indices are calculated as a percent of the averaged control; thus only db/db values are plotted and statistics are not performed. Coronary arteriole wall cell numbers were increased in db/db coronary arterioles when compared to control. Formalin fixed (constant gravity-fed perfusion) hearts were stained with α-smooth muscle actin and counter stained with DAPI. Cells with positive staining for both α-smooth muscle actin and DAPI were counted and then normalized to medial cross sectional area. Cumulative data from n=4 **(b)**. Values are mean SEM, * $p < 0.05$, vs. control.

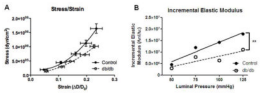

Fig. 4.

Decreased stress/strain relationship and stiffness of coronary arterioles isolated from 16-wk db/db vs. control. The db/db stress/stain curve was shifted to the right and the slopewas reduced indicating decreased vascular wall stiffness **(a)**. In addition, incremental elastic modulus was significantly reduced in db/db coronary arterioles **(b)**. Values are mean SEM, ** $p < 0.01$, vs. control.

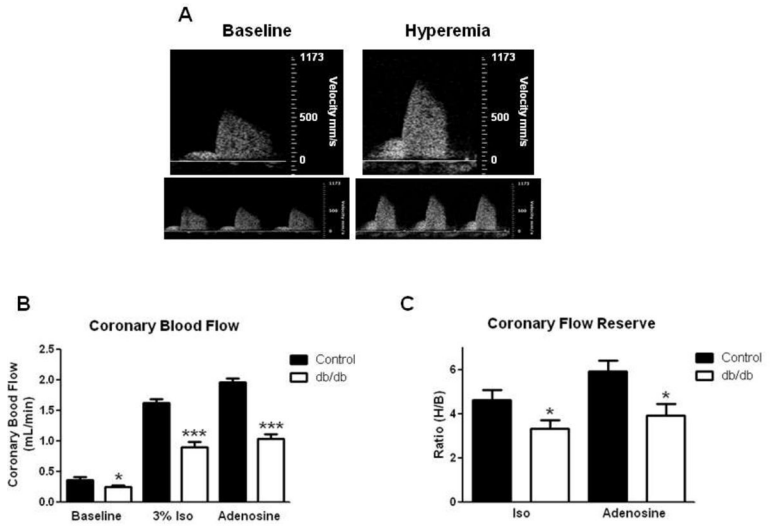

Fig. 5.

Representative pulse wave Doppler coronary flow curves demonstrating baseline and hyperemia flow **(a)**. Coronary blood flow was reduced in db/db mice at baseline and during hyperemic conditions using both 3% isoflurane and adenosine infusion (**b**). Coronary flow reserve was reduced in diabetic mice with either isoflurane or adenosine (**c**). Values are mean SEM, * $p < 0.05$, and *** $p < 0.001$ vs. control.

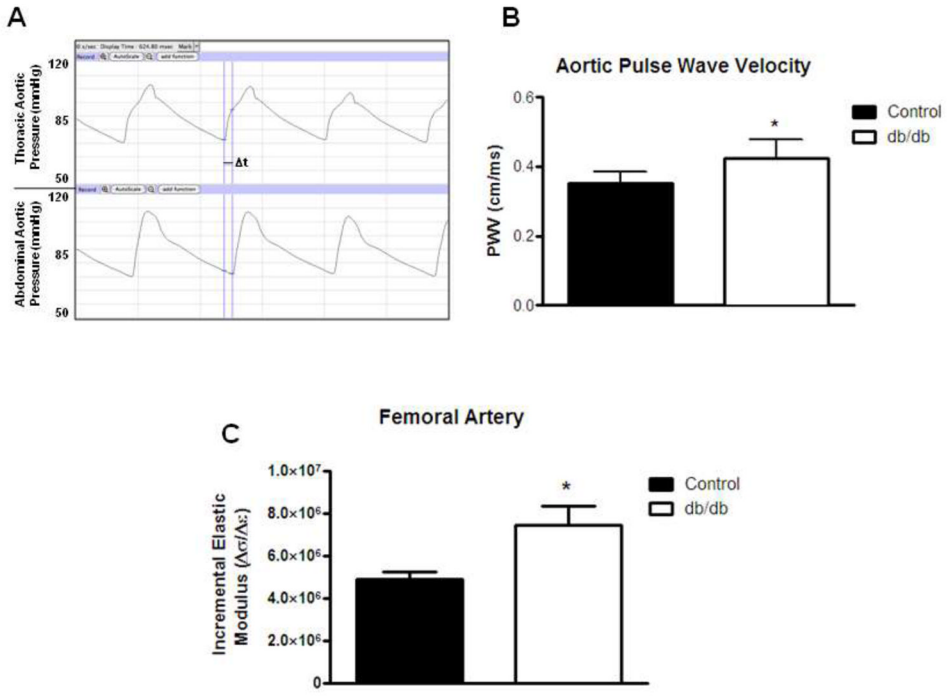

Fig. 6.

Aortic pulse wave velocities were measured in vivo using two pressure catheters, one placed in the thoracic aorta and one in the abdominal aorta. Representative tracings from each pressure catheter demonstrate the time delay between the thoracic and abdominal pressure tracings **(a)**. Aortic pulse wave velocities were calculated by dividing the distance between the pressure catheters (cm) by the time delay (s) and were increased db/db mice when compared to controls **(b)**. Increased stiffness of femoral arteries isolated from 16-wk db/db vs. control. Incremental elastic modulus calculated over a range of pressures (75–125 mmHg) was significantly increased in db/db femoral arteries **(c)**. Values are mean SEM, * $p < 0.05$ vs. control.

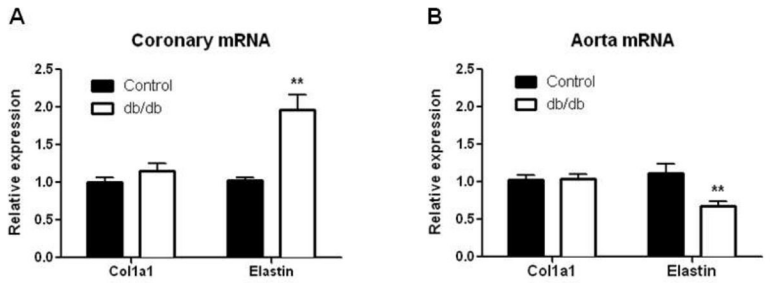

Fig. 7.

mRNA expression of col1a1 and elastin in 16-wk db/db coronary arterioles. mRNA expression was quantified by real-time PCR and normalized to the internal reference Rpl13A. Values are expressed as fold change (Control set to 1.0). Values are mean SEM, ** p <0.01 vs. control.

Table 1

PCR primers

Target	NCBI Accession #	Forward Primer	Reverse Primer	Roche Universal Probe #
Elastin	NM_007925	gctgatcctcttgctcaacc	gggaactccaccaggaagtc	64
Col 1a1	NM_007742	acctaagggtaccgctgga	gagctccagcttctccatctt	18
Rpl13a	NM_009438	tccctgctgctctcaagg	gccccaggtaagcaaactt	41

Table 2

Body weight, fasting blood glucose levels, and systolic blood pressure

	12-wks			16-wks		
	Control	**db/db**	***P* value**	**Control**	**db/db**	***P* value**
Body weight (g)	30 ± 1	49 ± 1	0.0001	33 ± 1	50 ± 2	0.0001
Fasting blood glucose (mg/dl)	122 ± 4	388 ± 25	0.0001	121 ± 6	394±50	0.0001
Systolic blood pressure (mm Hg)	-	-	-	128 ± 5	128 ± 3	>0.05
Diastolic blood pressure (mm Hg)	-	-	-	98 ± 5	99 ± 4	>0.05
Heart rate (beats per min)	-	-	-	435 ± 22	469 ± 17	>0.05

Values are mean SEM, p< 0.0001 db/db vs. control, t-test, n= 24 mice per group for blood glucose and body weight, n=6 mice per group for blood pressure and heart rate.

Table 3

Passive structural measurements of 12-wk mice

	Control	db/db	*P* value
Internal Lumen (μm)			
50 mm Hg	110 ± 6	94 ± 5	>0.05
75 mmHg	116 ± 6	101 ± 6	>0.05
100 MmHg	122 ± 6	106 ± 6	>0.05
Wall Thickness (μm)			
50 mm Hg	8 ± 1	8 ± 1	>0.05
75 mmHg	7 ± 1	7 ± 1	>0.05
100 MmHg	7 ± 1	7 ± 1	>0.05
Wall/Lumen			
50 mm Hg	7.6 ± 0.7	8.8 ± 0.6	>0.05
75 mmHg	6.4 ± 0.7	7.3 ± 0.6	>0.05
100 MmHg	5.7 ± 0.6	6.7 ± 0.7	>0.05
Medial Cross Sectional Area (μm^2)			
50 mm Hg	3059.2 ± 346.2	2688.2 ± 410.9	>0.05
75 mmHg	2862.7 ± 318.0	2547.3 ± 386.6	>0.05
100 MmHg	2745.8 ± 309.4	2507.5 ± 394.4	>0.05

Values are mean SEM, n= 8 mice per group.